Dense Matter Equation of State from Compact Object Mergers

J. M. Lattimer

Department of Physics & Astronomy

STONY BROOK UNIVERSITY

U.S. DEPARTMENT OF ENERGY
Office of Science

Solvay Workshop in honour of Michel Godefroid
'New Frontiers in Atomic, Nuclear, Plasma and Astrophysics'
Brussels, 25–27 November 2019

Acknowledgements

Funding Support:

US DOE - Nuclear Physics

US DOE - Toward Exascale Astrophysics of Mergers and Supernovae (TEAMS)

NASA - Neutron Star Interior Composition ExploreR (NICER)

NSF - Neutrinos, Nuclear Astrophysics and Symmetries (N3AS)

Recent Collaborators:

Duncan Brown & Soumi De (Syracuse), Christian Drischler (Berkeley), Evgeni Kolomeitsev (Matej Bei, Slovakia), Akira Ohnishi (YITP, Kyoto), Madappa Prakash (Ohio), Achim Schwenk (Darmstadt), Andrew Steiner (Tennessee), Ingo Tews (Los Alamos), Tianqi Zhao & Will Farr (Stony Brook)

Main Topics

- Neutron Stars and How They Depend on the Equation of State
- Measuring Neutron Star Properties From Radio and X-ray Observations
- Nuclear Physics Constraints on Neutron Stars and the Equation of State
- Estimating Neutron Star Properties from Neutron Star Mergers
- Where Do We Go From Here?

Dany Page
UNAM

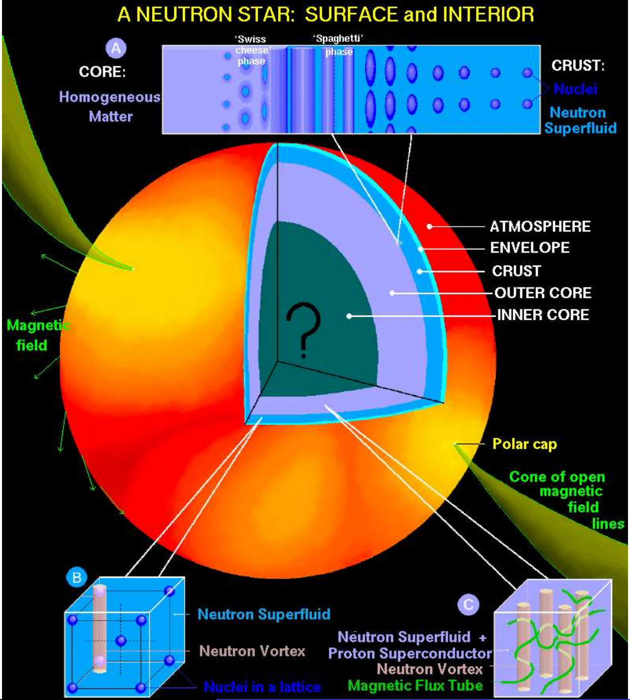

Neutron Star Structure

Tolman-Oppenheimer-Volkov equations

$$\frac{dp}{dr} = -\frac{G}{c^4}\frac{(mc^2 + 4\pi pr^3)(\varepsilon + p)}{r(r - 2Gm/c^2)}$$

$$\frac{dm}{dr} = 4\pi\frac{\varepsilon}{c^2}r^2$$

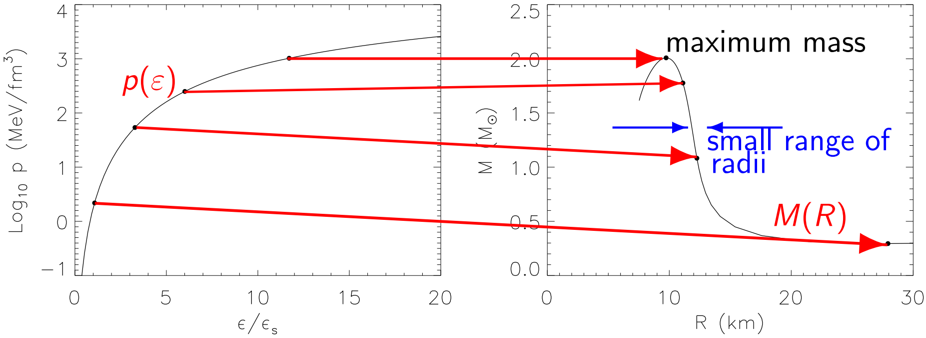

Equation of State ← Observations

Mass-Radius Diagram and Theoretical Constraints

GR:
$R > 2GM/c^2$

$P < \infty$:
$R > (9/4)GM/c^2$

causality:
$R \gtrsim 2.9GM/c^2$

— normal NS
— SQS

— $R_\infty = \frac{R}{\sqrt{1-2GM/Rc^2}}$

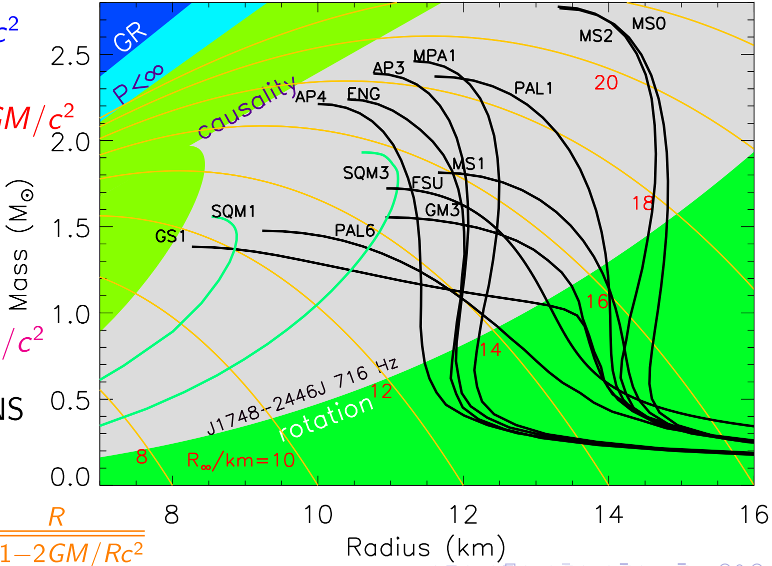

Nuclear Symmetry Energy and the Pressure

The symmetry energy is the difference between the energies of pure neutron matter ($x = 0$) and symmetric ($x = 1/2$) nuclear matter:

$$S(n) = E(n, x = 0) - E(n, x = 1/2)$$

Usually approximated as an expansion around the saturation density (n_s) and isopin symmetry ($x = 1/2$):

$$E(n, x) = E(n, 1/2) + (1-2x)^2 S_2(n) + \dots$$

$$S_2(n) = \mathbf{S_v} + \frac{\mathbf{L}}{3}\frac{n - n_s}{n_s} + \dots$$

$$\mathbf{S_v} \simeq 31 \text{ MeV}, \quad \mathbf{L} \simeq 50 \text{ MeV}$$

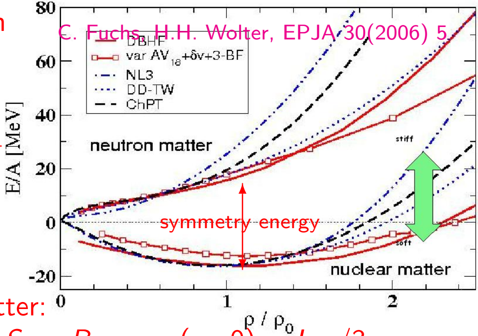

Extrapolated to pure neutron matter:

$$E(n_s, 0) \approx S_v + E(n_s, 1/2) \equiv S_v - B, \qquad p(n_s, 0) = L n_s/3$$

Neutron star matter (beta equilibrium) is nearly neutron matter:

$$\frac{\partial(E + E_e)}{\partial x} = 0, \quad p(n_s, x_\beta) \simeq \frac{L n_s}{3}\left[1 - \left(\frac{4S_v}{\hbar c}\right)^3 \frac{4 - 3S_v/L}{3\pi^2 n_s}\right]$$

Bounds From Unitary Gas Conjecture

Neutron matter energy should be larger than the unitary gas energy $E_{UG} = \xi_0 (3/5) E_F$

$$E_{UG} = 12.6 \left(\frac{n}{n_s}\right)^{2/3} \mathrm{MeV}$$

The unitary gas refers to fermions interacting via a pairwise short-range s-wave interaction with an infinite scattering length and zero range. Cold atom experiments show a universal behavior with the Bertsch parameter $\xi_0 \simeq 0.37$.

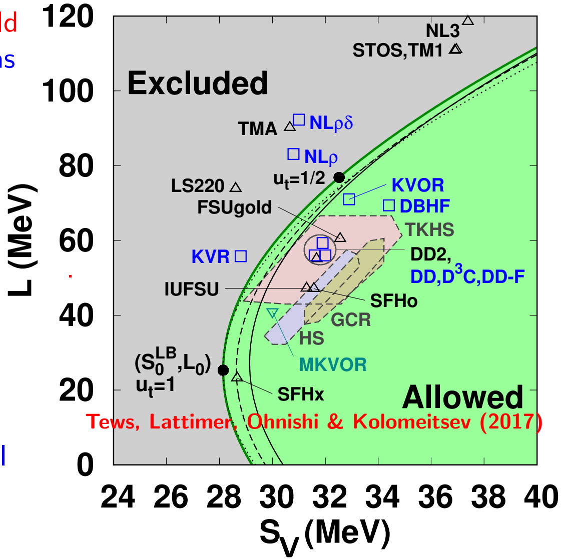

$S_v \geq 28.6$ MeV; $L \geq 25.3$ MeV; $p_0(n_s) \geq 1.35$ MeV fm^{-3}; $R_{1.4} \geq 9.7$ km

Nuclear Experimental Constraints

Neutron Skin Thickness

$$r_{np} = \frac{2r_o}{3S_v}\frac{1}{\sqrt{1-I^2}}(1+S_sA^{-1/3}/S_v)^{-1}$$
$$\times\sqrt{\frac{3}{5}}\left[IS_s - \frac{3Ze^2}{140r_o}\left(1+\frac{10}{3}\frac{S_sA^{-1/3}}{S_v}\right)\right]$$

$$r_{np,208} = 0.15 \pm 0.04 \text{ fm}$$

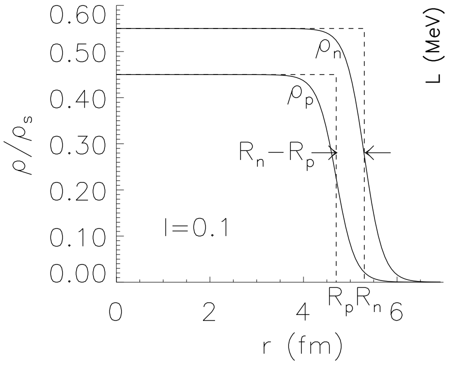

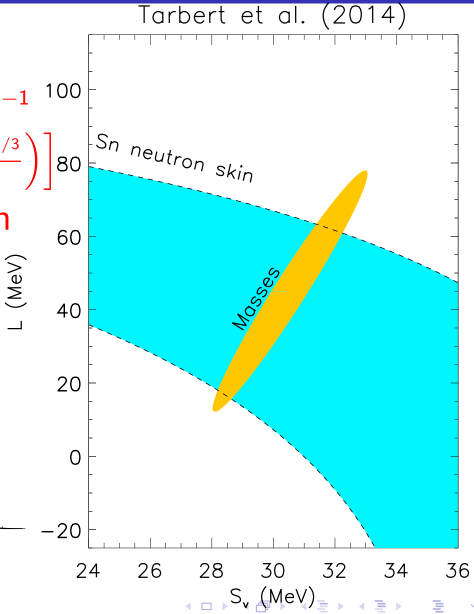

Theoretical and Experimental Constraints

H Chiral Lagrangian

G: Quantum Monte Carlo

neutron matter calculations from Hebeler et al. (2012)

unitary gas constraints from Tews et al. (2017)

Combined experimental constraints are compatible with unitary gas bounds.

Neutron matter calculations are compatible with both.

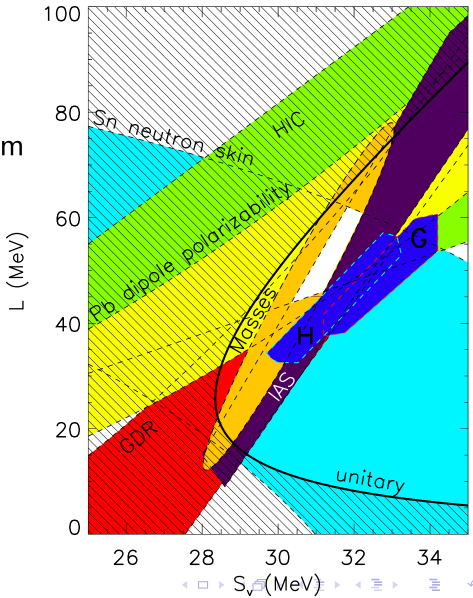

The Radius – Pressure Correlation

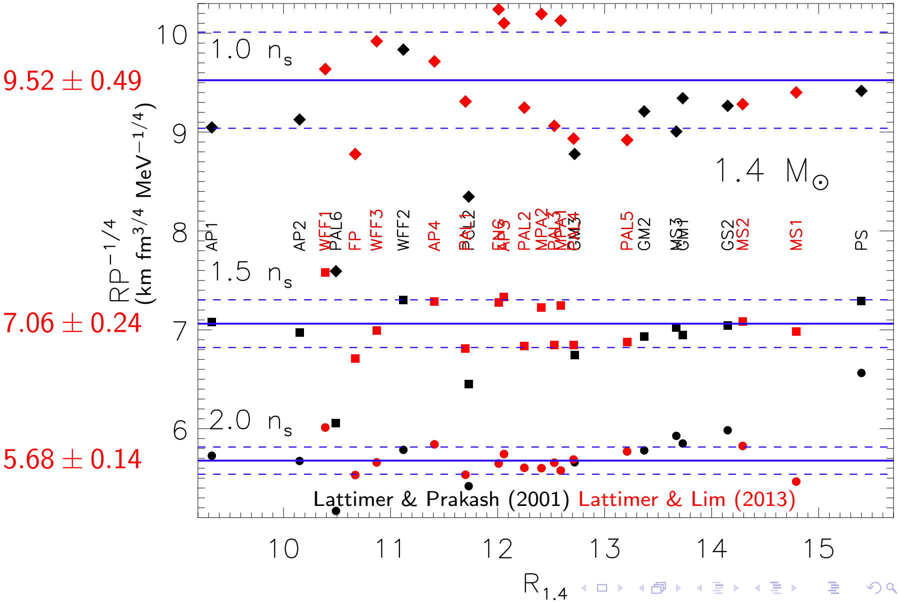

Theoretical and Experimental Constraint Summary

$$R_{1.4} = (9.52 \pm 0.49) \left(\frac{p_s}{\mathrm{MeV\ fm}^{-3}} \right)^{1/4} \mathrm{km}$$

$$p_s \simeq n_s L/3$$

$$30\ \mathrm{MeV} \lesssim L \lesssim 70\ \mathrm{MeV}:$$

$$10.9\ \mathrm{km} \lesssim R_{1.4} \lesssim 13.1\ \mathrm{km}$$

Causality and $M_{max} \gtrsim 2.0 M_\odot$: $R_{1.4} \gtrsim 8.2\ \mathrm{km}$
Imposing the unitary gas conjecture: $R_{1.4} \gtrsim 9.7\ \mathrm{km}$

How to Measure Neutron Star Masses and Radii

- Pulsar timing can accurately ($\gtrsim 0.0001 M_\odot$) measure masses.

  Most are between $1.2 M_\odot$ and $1.5 M_\odot$; lowest is $1.174 \pm 0.004 M_\odot$, highest are $2.14^{+0.10}_{-0.09} M_\odot$ and $2.01 \pm 0.04 M_\odot$. Higher estimates have large uncertainties.

- Thermal and bursting observations of X-rays yield radii, but uncertain to a few km.
  - Quiescent sources in globular clusters
  - Thermonuclear explosions on accreting neutron stars in binaries
  - Pulse profile modeling of hot spots on rapidly rotating neutron stars (NICER experiment)

- Gravitational waves from merging neutron stars measure masses and tidal deformabilites.

  GW170817 suggests $R = 11 \pm 1$ km

GW170817

- LIGO-Virgo (LVC) detected a signal consistent with a BNS merger, followed 1.7 s later by a weak sGRB.
- 16600 orbits observed over 165 s.
- $\mathcal{M} = 1.187 \pm 0.001\ M_\odot$
- $M_{\rm T,min} = 2^{6/5}\mathcal{M} = 2.726 M_\odot$
- $E_{\rm GW} > 0.025 M_\odot c^2$
- $D_L = 40 \pm 10$ Mpc
- $75 < \tilde{\Lambda} < 560$ (90%)
- $M_{\rm ejecta} \sim 0.06 \pm 0.02\ M_\odot$
- Blue ejecta: $\sim 0.01 M_\odot$
- Red ejecta: $\sim 0.05 M_\odot$
- Possible r-process production
- Ejecta + GRB: $M_{max} \lesssim 2.2 M_\odot$

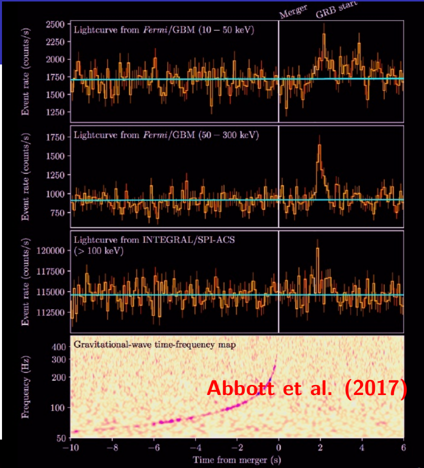

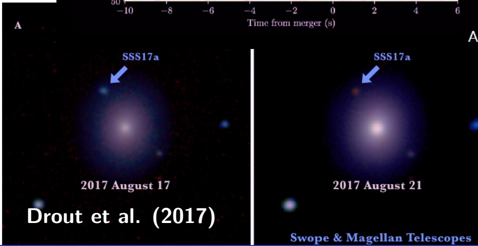

Properties of Known Double Neutron Star Binaries

- Both component masses are accurately measured (11)

— Only the total binary mass is accurately measured (7)

Binaries with $\tau_{GW} > t_{\rm universe}$ (6)

$q = M_2/M_1$ is the binary mass ratio for a system

$\chi = cJ/(GM^2)$ is the dimensionless spin parameter for individual pulsars

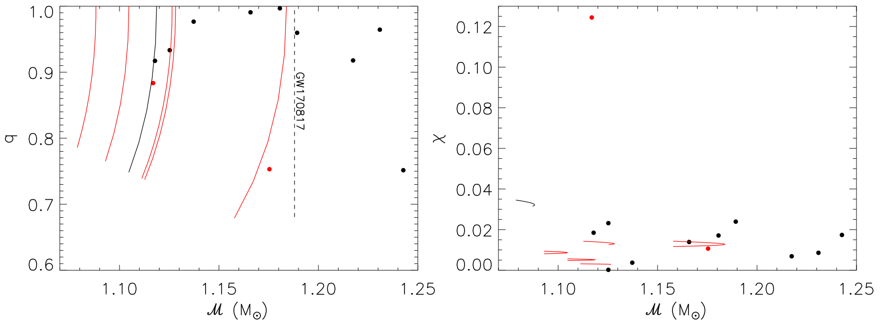

$\mathcal{M} = (M_1 M_2)^{3/5}(M_1 + M_2)^{-1/5}$ is the chirp mass

Binary Pulsar Decay Time Distribution

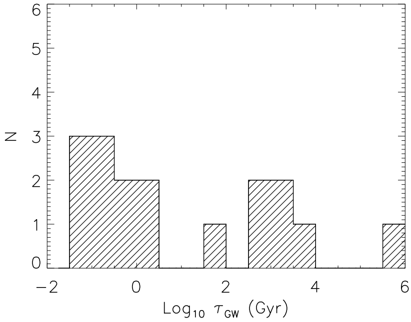

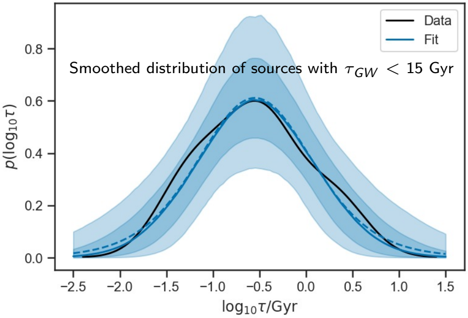

16% have $\tau_{GW} < 90$ Myrs.

33% have $\tau_{GW} < 150$ Myrs.

This evidence could support mergers as the primary *r*-process source.

Waveform Model Parameters

There are 13 wave-form free parameters including finite-size effects at third PN order $(v/c)^6$. LVC17 used a 13-parameter model; De et al. (2018) used a 9-10 parameter model.

- Sky location (2) EM data
- Distance (1) EM data
- Inclination (1)
- Coalescence time (1)
- Coalescence phase (1)
- Polarization (1)

} Extrinsic

- Component masses (2)
- Spin parameters (2)
- Tidal deformabilities (2) correlated with masses

} Intrinsic

Tidal Deformability

The tidal deformability λ is the ratio of the induced dipole moment Q_{ij} to the external tidal field E_{ij}, $Q_{ij} \equiv -\lambda E_{ij}$.

Work with the dimensionless quantity

$$\Lambda = \frac{\lambda c^{10}}{G^4 M^5} \equiv \frac{2}{3} k_2 \left(\frac{Rc^2}{GM}\right)^5$$

k_2 is the dimensionless Love number.

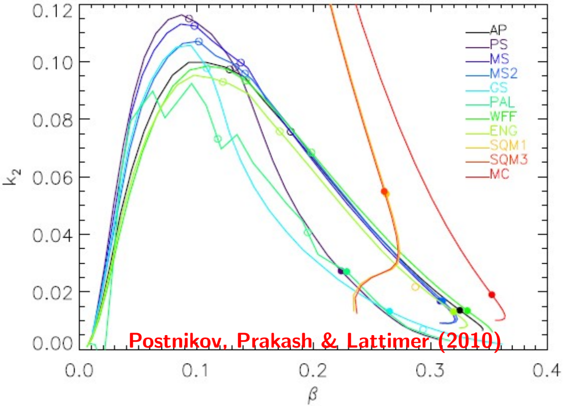

For a neutron star binary, $\tilde{\Lambda}$ is the relevant quantity:

$$\tilde{\Lambda} = \frac{16}{13}\frac{(1+12q)\Lambda_1 + (12+q)q^4\Lambda_2}{(1+q)^5}, \qquad q = M_2/M_1 \le 1$$

The Effect of Tides

Tides accelerate the inspiral and produce a phase shift compared to the case of two point masses.

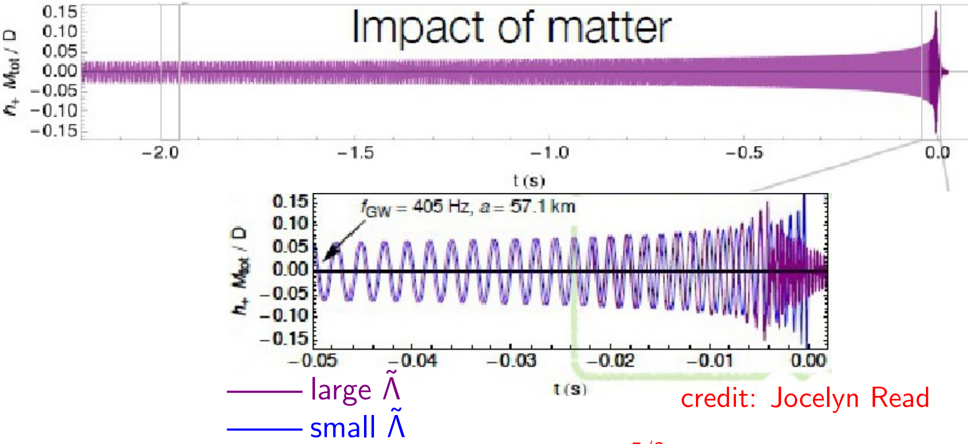

credit: Jocelyn Read

$$\delta\Phi_t = -\frac{117}{256}\frac{(1+q)^4}{q^2}\left(\frac{\pi f_{GW} G\mathcal{M}}{c^3}\right)^{5/3}\tilde{\Lambda} + \cdots .$$

Λ is Highly Correlated With M and R

- $\Lambda = a\beta^{-6}$
  $\beta = GM/Rc^2$

  $a = 0.0086 \pm 0.0011$
  for
  $M = 1.35 \pm 0.25\ M_\odot$

- If $R_1 \simeq R_2 \simeq R_{1.4}$
  it follows that
  $\Lambda_2 \simeq q^{-6}\Lambda_1$.

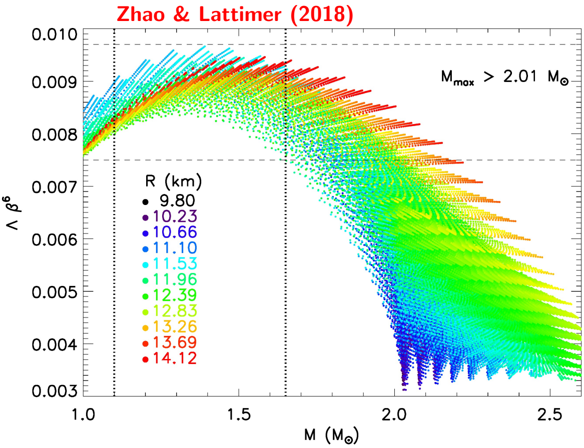

Binary Deformability and the Radius

$$\tilde{\Lambda}=\frac{16}{13}\frac{(1+12q)\Lambda_1+q^4(12+q)\Lambda_2}{(1+q)^5}\simeq\frac{16a}{13}\left(\frac{R_{1.4}c^2}{G\mathcal{M}}\right)^6\frac{q^{8/5}(12-11q+12q^2)}{(1+q)^{26/5}}$$

- $\tilde{\Lambda}=a'(R_{1.4}c^2/G\mathcal{M})^6$
  $a'=0.0035\pm0.0006$
  for
  $\mathcal{M}=1.2\pm0.2\ M_\odot$
- GW10817:
  $a'=0.00375\pm0.00025$
- $R_{1.4}=$
  $11.5\pm0.3\ \frac{\mathcal{M}}{M_\odot}\left(\frac{\tilde{\Lambda}}{800}\right)^{1/6}$ km
- GW10817:
  $R_{1.4}=13.4\pm0.1\ \left(\frac{\tilde{\Lambda}}{800}\right)^{1/6}$ km

Zhao & Lattimer (2018)

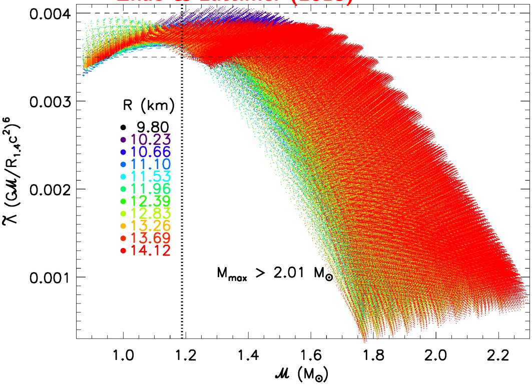

Re-Analysis of GW170817 (De et al. 2018)

- De18 takes advantage of the precisely-known electromagnetic source position (Soares-Santos et al. 2017).
- Uses existing knowledge of H_0 and the redshift of NGC 4993 to fix the distance (Cantiello et al. 2017).
- Assumes both neutron stars have the same equation of state, which implies $\Lambda_1 \simeq q^6 \Lambda_2$.
- Baseline model effectively has 9 instead of 13 parameters.
- Explores variations of mass, spin and deformability priors.
- Low-frequency cutoff taken to be 20 Hz, not 30 Hz as in LVC17, doubling the number of analyzed orbits.

De18 find that including $\Lambda - M$ correlations

- establishes a lower 90% confidence bound to $\tilde{\Lambda}$ (which is above the causal minimum value), and
- reduces the upper 90% confidence bound to $\tilde{\Lambda}$ by 30%.

68%, 80%, 90% and 95% Confidence Bounds

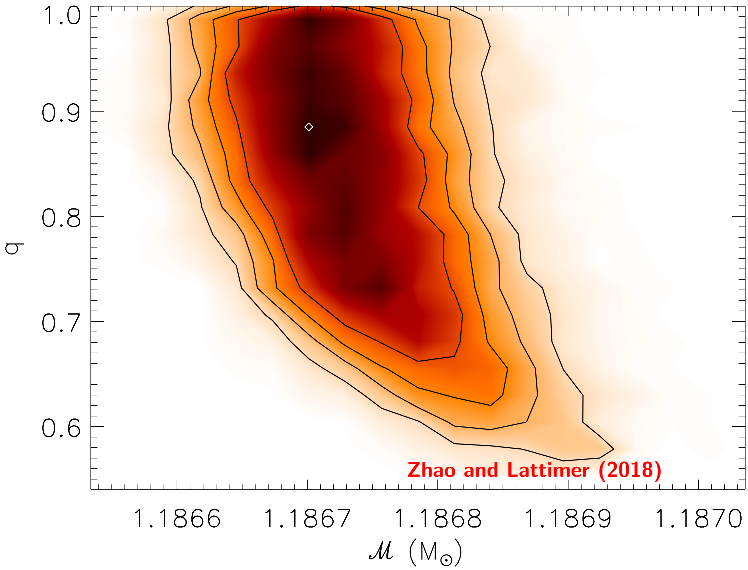

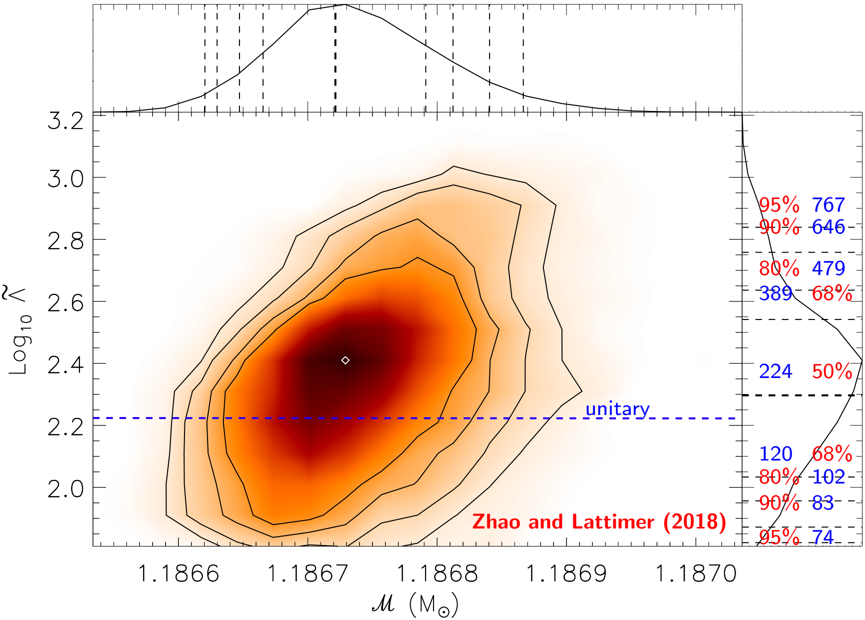

3.2
3.0
2.8
2.6
2.4
2.2
2.0
$\mathrm{Log}_{10}\,\tilde{\Lambda}$
1.1866
1.1867
1.1868
1.1869
1.1870
$\mathcal{M}$ ($M_\odot$)
unitary
Zhao and Lattimer (2018)
95% 767
90% 646
80% 479
389 68%
224 50%
120 68%
80% 102
90% 83
95% 74

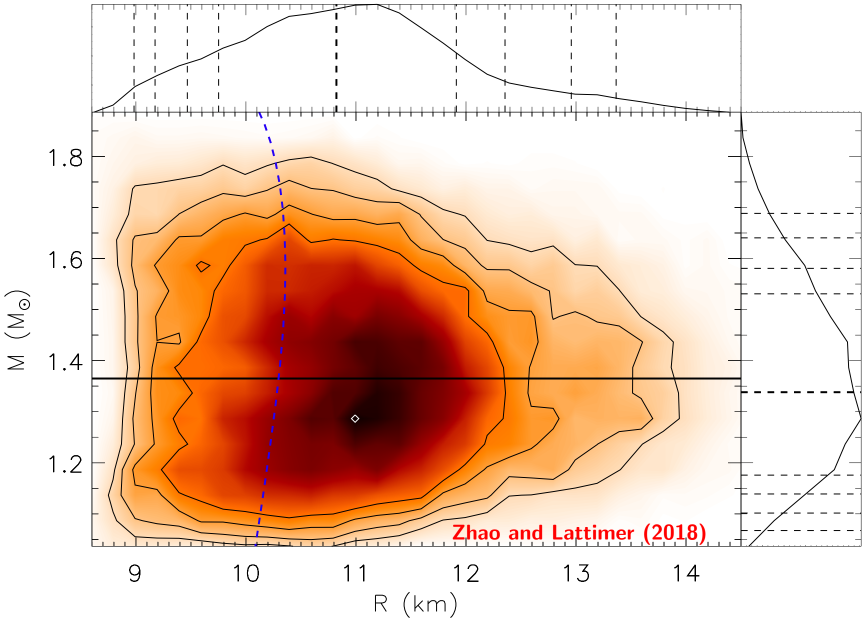

1.8
1.6
1.4
1.2
M (M⊙)
9
10
11
12
13
14
R (km)
Zhao and Lattimer (2018)

$M - R$ With UG and Uniform R Priors

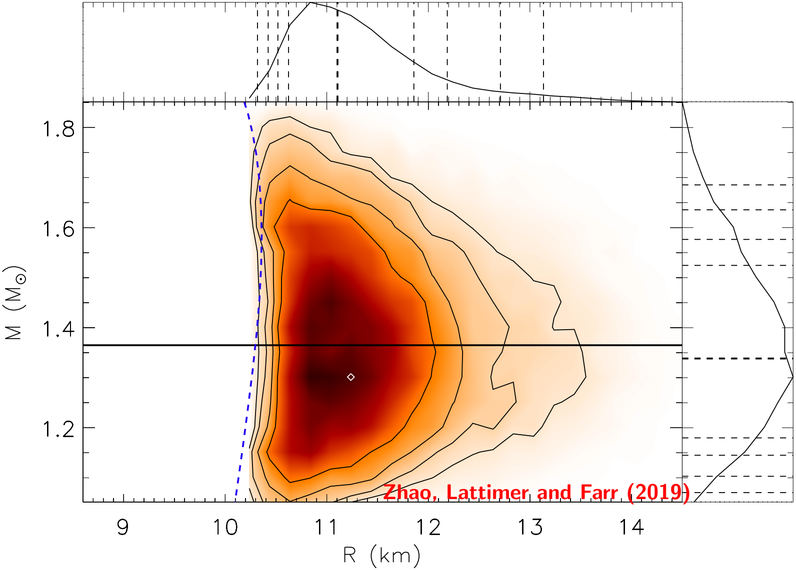

$M - R$ With No $\Lambda - M$ Correlations

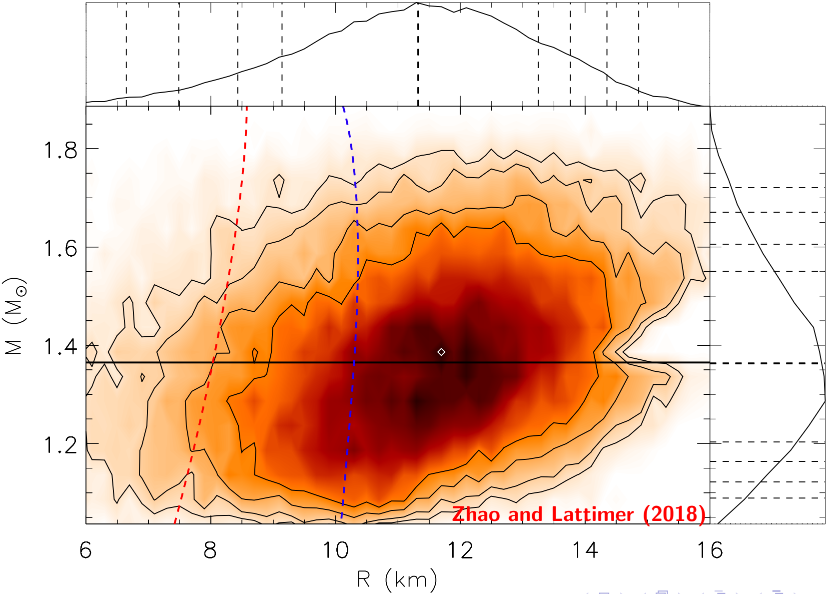

Maximum Mass Constraint From GW170817

- Pulsar observations imply non-rotating $M_{max} \gtrsim 2M_\odot$.
- Remnant differential rotation uniformizes within ~ 0.1s.
- Inspiralling mass $M_T = \mathcal{M} q^{-3/5}(1+q)^{6/5}$ is $2.73M_\odot$ ($q=1$) to $2.78M_\odot$ ($q=0.7$), smaller than $M_{max,d}$.
- Maximally uniformly rotating stars have $M_{max,u} = \xi M_{max}$ with $1.17 \lesssim \xi \lesssim 1.21$. *Hypermassive* stars, with $M_T > M_{max,u}$, promptly collapse to a BH.
- *Supermassive* stars, with $M_{max} \le M_T \le M_{max,u}$, are metastable but have much longer lifetimes. Such a remnant pumps too much energy into the ejecta to be consistent with observations.
- Taking into account gravitational binding energy, the condition $M_T > M_{max,u}$ implies $M_{max} \le 2.25M_\odot$.

LVC O3 Detections To Date (5 Months)

23 binary black hole systems, of which 1 is marginal.

4 binary neutron star systems, of which 2 are marginal.

- S190425z (156 $\pm$ 41 Mpc, FAR $= 4.5 \cdot 10^{-13}$)
- S190510g (1331 $\pm$ 341 Mpc, FAR $= 8.8 \cdot 10^{-10}$)
- S190901ap (241 $\pm$ 79 Mpc, FAR $= 7.0 \cdot 10^{-9}$)
- S190910h (241 $\pm$ 89 Mpc, FAR $= 3.6 \cdot 10^{-8}$)

3 black hole-neutron star systems, of which 1 is marginal.

- S190426c (377 $\pm$ 100 Mpc, FAR $= 1.9 \cdot 10^{-8}$)
- S190814bv (267 $\pm$ 52 Mpc, FAR$=2.0 \cdot 10^{-33}$)
  $p_{\rm BHNS} = 0.998$, $p_{\rm gap} = 0.002$
- S190910d (632 $\pm$ 186 Mpc, FAR $= 3.7 \cdot 10^{-9}$)
  $p_{\rm BHNS} = 1.000$

Summary

- GW170817 provided R and EOS information compatible with expectations from nuclear theory, experiment and other astrophysical observations, considering existing systematic uncertainties.
- GW170817 also hints that M_{max} is not far above the minimum provided by pulsar timing.
- NICER should soon provide complementary radius information from X-ray sources.
- Future GW measurements will be additive since BNS sources should be similar.